Available online at www.sciencedirect.com
ScienceDirect
Journal of Photochemistry and Photobiology A: Chemistry 197 (2008) 1–12
Journal of Photochemistry and Photobiology A:Chemistry
www.elsevier.com/locate/jphotochem

Light-induced effects in sulfonated aluminum phthalocyanines—potential photosensitizers in the photodynamic therapy Spectroscopic and kinetic study

Krystyna Palewska [a,*], Marta Sujka [a,1], Barbara Urasińska-Wójcik [a,2], Juliusz Sworakowski [a], Józef Lipiński [a], Stanislav Nešpůrek [b], Jan Rakušan [c], Marie Karásková [c]

[a] *Institute of Physical and Theoretical Chemistry, Wrocław University of Technology, Wyb. Wyspiańskiego 27, 50-370 Wrocław, Poland*
[b] *Institute of Macromolecular Chemistry AS CR, v. v. i., Heyrovský Sq. 2, 162 06 Prague 6, Czech Republic*
[c] *Research Institute of Organic Synthesis, 532 18 Pardubice-Rybitví, Czech Republic*

Received 20 September 2007; received in revised form 26 November 2007; accepted 28 November 2007
Available online 3 December 2007

Abstract

Sodium salts of sulfonated hydroxyaluminum phthalocyanines [Al(OH)Pc(SO_3Na)$_i$] containing various numbers of sulfonate groups (i = 1–4), were studied by spectroscopic techniques. The lifetimes of the singlet states were found to range between 5 and 8 ns, experimentally determined fluorescence quantum yields ranging between 0.45 and 0.74. Both parameters depend on the number of sulfonate groups, the singlet lifetime depending additionally on concentration. The triplet lifetime was indirectly estimated for aqueous solutions of Al(OH)Pc(SO_3Na)$_3$ to amount to ca. 0.6 μs. The decay time of singlet oxygen in the same system was also found to be close to 0.6 μs. The molecules were found to dimerize in acidic and neutral solutions, the second order rate constants of the dimerization being of the order of 10 mol^{-1} dm^3 s^{-1}, and the equilibrium constants of the order of 10^4. The experiments were supplemented with quantum chemical calculations allowing us to assign electronic transitions in monomers and dimers.

Keywords: Aluminum phthalocyanine; Absorption spectra; Emission spectra; Dimerization; Photodynamic therapy

1. Introduction

Cancerous tumors are conventionally treated with radiation therapy, chemotherapy or surgery but these methods have often life threatening side effects. Photodynamic therapy (PDT) offers an alternative for the treatment of cancer, employing a combination of light and a drug (called photosensitizer) to selectively destroy tumor tissue. Upon activation with light, the photosensitizer is excited to a higher electronic state, and after energy transfer induces formation of cytotoxic agents. Ideally, the photosensitizer is localized in or around the tumor tissue, is non-toxic to normal tissues and is photochemically efficient in producing cytotoxic agents [1–3]. The benefits of PDT are that (i) following the treatment, the affected areas heal with regeneration of normal tissue, (ii) it can be used, if necessary, in conjunction with conventional cancer therapies, (iii) photosensitizer fluorescence enables *in vivo* detection and localization of neoplastic tissue on a microscopic scale and provides a convenient tool for monitoring its concentration [4,5].

The treatment involves the intravenous injection of a sensitizer which is quickly transported to all tissues. The illumination of the sensitizer leads usually to the formation of radicals (Type I reactions) or of singlet oxygen (Type II reactions) (see Fig. 1a). An extensive review on photosensitized singlet oxygen has been published in [6].

Many sensitizers have been tested for PDT, photogeneration of singlet oxygen or ion-radicals. In particular, many new "second generation drugs" have been synthesized in recent years, mostly based on a cyclic tetrapyrrole structure with intensi-

* Corresponding author. Tel.: +48 71 320 3227; fax: +48 71 320 3364.
E-mail address: krystyna.palewska@pwr.wroc.pl (K. Palewska).
[1] Present address: Institute of Food Research, Norwich Research Park, Colney, Norwich NR4 7UA, UK.
[2] Present address: The Nanomaterials Group, School of Chemistry, University of Wales, Bangor, Deiniol Street, Bangor, Gwynedd LL55 2UW, UK.

1010-6030/$ – see front matter © 2007 Elsevier B.V. All rights reserved.
doi:10.1016/j.jphotochem.2007.11.025

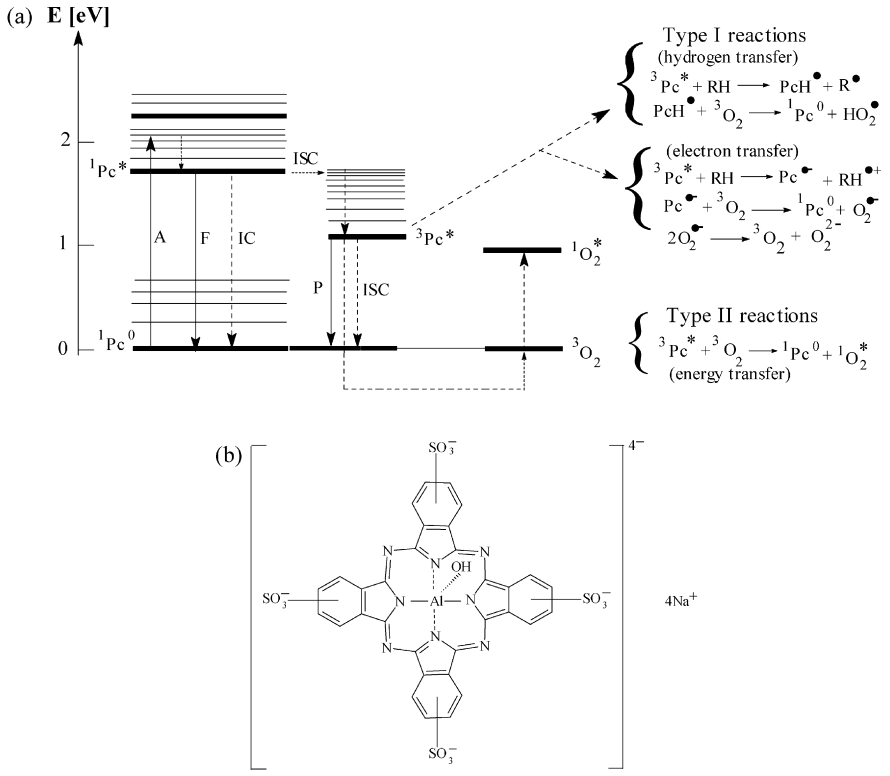

Fig. 1. (a) Jablonski diagram and scheme of reaction mechanisms between a phthalocyanine molecule (acting as a photosynthesizer) and oxygen. (b) Formula of sodium salt of tetrasulfonated phthalocyanine $(Al(OH)PcS_4)^{4-}$ $4Na^+$.

fied and red shifted absorption spectra. Here, one can mention phthalocyanines (Pc) [7] (cf. Fig. 1b). Due to the extended conjugation of the pyrrole moieties, Pcs exhibit very strong absorption bands near 670 nm and are essentially transparent between 400 and 600 nm. These compounds allow deeper light penetration of tissue and are substantially less efficient in inducing skin photosensitivity.

The stability of metal phthalocyanines is due to formation of four equivalent N → metal σ bonds involving filling of vacant *n*s, *n*p, and $(n-1)$d or *n*d orbitals of the cation with σ electrons of the central nitrogen atoms. The nature of the central metal influences photophysical properties of phthalocyanines, among them the quantum yield of the formation of the triplet state and its lifetime. Pcs with open shell or paramagnetic metal ions such as Cu^{2+}, Co^{2+}, Fe^{2+}, Ni^{2+}, V^{2+}, Cr^{3+} and Pd^{2+} exhibit short triplet lifetimes (submicrosecond range) due to increased intersystem crossing back to the ground state, which renders the dye photoinactive [8]. Pcs containing closed d shell or diamagnetic metal ions, such as Zn^{2+}, Al^{3+} and Ga^{3+}, are dyes exhibiting high triplet yields ($\phi_T > 0.4$) with long triplet lifetimes in the micro- and millisecond range ($\tau_T > 200$ μs) [9]. The energies of triplets, exceeding 1.14 eV (110 kJ mol^{-1}) [10], are sufficient to generate singlet oxygen ($E_{^1O_2} \approx 94$ kJ mol^{-1}, i.e., ∼0.97 eV). A reasonable triplet state quantum yield ($\phi \approx 0.3$–0.5 depending on the nature of central ligands and side groups attached to the peripheral rings) has been reported [11,12].

Nearly all unsubstituted Pcs are insoluble, the solubility being introduced by attaching suitable side groups. In particular, substitution with hydrophilic groups results in obtaining Pcs soluble in aqueous solutions. In these solutions, however, Pcs tend to aggregate, in consequence losing their photochemical activity because excitation of an aggregate is preferentially followed by the internal conversion to the ground state [9].

In this work, we present results of a study of properties of a family of sodium salts of sulfonated hydroxyaluminum phthalocyanines ($[Al(OH)Pc(SO_3Na)_i]$, hereafter referred to as $Al(OH)PcS_i$—cf. Fig. 1b) containing various numbers of sulfonate groups ($i = 1$–4). These water soluble compounds are considered promising second generation drugs as they show excellent photodynamic activity [13]. Their principal advantage over porphyrin sensitizers lies in their stronger absorption at longer wavelengths, near 700 nm ($\varepsilon \sim 10^5$ dm^3 mol^{-1} cm^{-1}). Measurements of absorption and emission spectra allowed us to determine their photochemical and photophysical properties. As photosensitizers should exhibit their activity in aqueous solutions of salts and proteins, studies of their properties in function of pH are important.

Absorption spectra were also used to study the kinetics of dimerization and the dimerization equilibria.

2. Experimental and calculations

2.1. Materials

Sodium salts of sulfonated hydroxyaluminum phthalocyanine $[Al(OH)Pc(SO_3Na)_i]$, $i = 1$–4, Fig. 1b) were synthesized from hydroxyaluminum phthalocyanine [Al(OH)Pc].

The sulfonation process was carried out in the four necked glass flask, heated in an oil bath and equipped with reflux cooler, agitator, thermometer and dosing funnel. 300 g of fuming sulfuric acid was charged into the flask and subsequently 30 g of Al(OH)Pc was gradually charged through the dosing funnel into the agitated fuming sulfuric acid. The mixture was agitated at 30 °C until all the Al(OH)Pc was fully dissolved. After that, the dosing funnel was removed and an inlet of nitrogen was installed instead of it. The process of sulfonation was carried out under the nitrogen blanket. The reaction mixture was agitated and heated up to a temperature between 115 and 125 °C, and subsequently kept for 30 min at the adjusted temperature. The concentration of fuming sulfuric acid and the temperature of the sulfonation were chosen according for the target level of the sulfonation. Lower sulfonated (mostly mono- and disulfonated) phthalocyanines were obtained when 5% fuming sulfuric acid was used at temperature 115 °C, whereas higher sulfonated (mostly di- and trisulfonated) phthalocyanines were obtained with 6% fuming sulfuric acid, at 125 °C. In the former case, the final product contained ca. 36% of mono- and 53% of disubstituted phthalocyanine, whereas in the latter case, the contents of di- and trisulfonated phthalocyanines amounted to 28% and 54%, respectively.

After the sulfonation process was terminated, the reaction mixture was slowly cooled down to laboratory temperature and subsequently charged with a drooping funnel into the vigorously agitated mixture of 2000 g of ice and 1000 g of water. The water suspension was then filtered with a Buchner funnel, the filter cake was washed with distilled water until no sulfate anions were detectable in the filtrate. Thoroughly washed filter cake of sulfonated Al(OH)PcS$_i$ was dried in laboratory dryer at 105 °C until the constant weight. The contents of particular sulfonated Al(OH)PcS$_i$ were determined by HPLC. The dry product of the sulfonation was always a mixture mono-, di-, tri- and tetrasulfonated aluminum phthalocyanines. In order to obtain mono-, di-, tri- and tetrasulfonated Al(OH)PcS$_i$, the mixtures of sulfonated derivatives, prepared as described above, were separated by the column liquid chromatography. The glass chromatographic column was filled with silica gel (Kieselgel 60 für die Säulen-Chrom Merck), the mixture of ethyl acetate, ethanol and 25% ammonia water (in the volume ratios 7:4:4) being used as a mobile phase. The purity of each dry product was determined by HPLC method, combined with mass spectrometry, which proved the molecular constitution of each separated phase. The purities of the materials under study are given in Table 1. It should be noted that two isomers can exist in Al(OH)PcS$_2$, differing in the relative positions of the sulfonate groups: *cis* (the groups attached to the vicinal rings) and *trans* (the groups attached to the opposite groups). Presently, there is no method of separating the two isomers of Al(OH)PcS$_2$. The value in the table refers to the purity of the mixture.

Table 1
Purities of sodium salts of sulfonated hydroxyaluminum phthalocyanines

Sample[a]	Purity (wt.%)
Al(OH)PcS$_1$	97.9
Al(OH)PcS$_2$[b]	99.4
Al(OH)PcS$_3$	98.6
Al(OH)PcS$_4$	98.2

[a] S stands for (SO_3Na).
[b] Purity of a mixture of *trans* and *cis* isomers.

It is important to note that the solubilities of the purified products depend on the number of sulfonate groups: Al(OH)PcS$_1$ was found to be reasonably soluble only in alkaline buffers, whereas Al(OH)PcS$_4$ could be dissolved even in acidic solutions.

2.2. Methods

Solutions were prepared using buffers at several pH values ranging between 2 and 12. The measurements were also taken in pure air-saturated water, and in a 1:1 mixture of methanol and 0.1 M NaOH. The concentration of the solutions varied from 10^{-7} to 10^{-4} M.[3]

Measurements of UV–vis absorption and fluorescence spectra of Al(OH)PcS$_i$ in solutions were carried out using Shimadzu UV-2101 PC spectrometer and Hitachi F-4500 fluorescence spectrophotometer, respectively. The fluorescence emission and excitation spectra were measured at both, 77 K and room temperature.

The fluorescence quantum yields of Al(OH)PcS$_i$ in solutions were measured in reference to a standard sample whose quantum yield had been previously determined by absolute measurements [14]. We employed the procedure recommended in [15]. The quantum yields of the samples under investigation (Φ_s) were calculated from the equation

$$\Phi_s = \frac{w_s n_{ref}^2 A_{ref}}{w_{ref} n_s^2 A_s} \Phi_{ref} \quad (1)$$

in which Φ_{ref} is the fluorescence quantum yield of the reference sample, n, w, and A stand for the refractive index, the area under the emission spectrum and the absorbance at the excitation wavelength, and the subscripts s and ref refer to the measured and to the reference samples, respectively. We used a solution of zinc phthalocyanine in (toluene + 1% pyridine) as the reference ($\Phi_{ref} = 0.3$) [10].

The singlet lifetime measurements were obtained by the single-photon method using a IBH Data Station Hub spectrofluorometer. All samples were excited at 360 nm and emission was recorded at 700 nm; a change of the emission wavelength resulted in insignificant changes of lifetimes. Triangular cuvettes were used in quantum yield and lifetime measurements.

Phosphorescence spectra were measured mainly at 77 K, in a 1:1 mixture of methanol and 0.1 M NaOH (pH 12). Attempts were also made to measure the phosphorescence spectra and triplet lifetimes at room temperature but, due to extremely low signal, no reliable results were obtained. The kinetics of formation and decay of singlet oxygen was measured thanks to the courtesy of Prof. J. Hála (Charles University Prague). Experimental details were identical as those described in [16].

[3] M ≡ mol dm^{-3}; this abbreviation will be used throughout the text.

2.3. Quantum-mechanical calculations

The experimental results were supplemented with quantum-chemical calculations. In the calculations, initial ground-state geometries of all aluminum phthalocyanines were obtained using the INDO [17] Hamiltonian. Next, these structures were re-optimized at the DFT level with the hybrid B3LYP exchange-correlation functional and the 6-31G* basis set [18]. Excitation energies and oscillator strengths (in the dipole length approximation) were calculated using the time dependent DFT (TDDFT) method implemented in the Gaussian 03 package [18] and the singly excited configuration interaction (CIS) approximation in our locally modified NDO-like method (GRINDOL program) in which one-electron Hamiltonian matrix elements are calculated from semi-theoretical formulae derived from Heisenberg equation of motion (for details see [19–21]).

3. Results

3.1. UV–vis absorption spectra

Typical absorption spectra of the sulfonated phthalocyanines under study are shown in Fig. 2a. The spectra consist of two main features, Soret (B) band and Q band centered around 350 and 670 nm, respectively, with a vibrational sideband observed around 610 nm. Another clearly distinguishable band, appearing at ca. 640 nm, is due to the presence of aggregates (dimers), possibly overlapping with a vibrational sideband (*vide infra*).

The exact positions of the principal bands depend on pH as is shown in Fig. 2b: the maxima of the Q band move by ca. 200 cm^{-1} towards higher energies on passing from acidic to alkaline solutions. For the Soret band, the respective shift is larger and amounts to ca. 500 cm^{-1}. The molar absorbances in the maxima of Q bands (determined in a pH 12 buffer) ranged between $1.0 \times 10^5\ M^{-1}\ cm^{-1}$ in $Al(OH)PcS_{1–3}$ and $1.6 \times 10^5\ M^{-1}\ cm^{-1}$ in $Al(OH)PcS_4$, and decreased on passing from alkaline to acidic solutions. Additionally, the Q-band of $Al(OH)PcS_i$ with odd number of the sulfonate groups is split and the presence of double peaks in the Q band region of the non-aggregated $Al(OH)PcS_1$ and $Al(OH)PcS_3$ are observed (see Fig. 2a). In alkaline solutions, in which both, $Al(OH)PcS_1$ and $Al(OH)PcS_3$ are soluble, the splitting is similar and amounts to 260 cm^{-1}. In $Al(OH)PcS_3$, where reliable measurements could be performed over a wide pH range, the splitting slightly increases with pH, being equal to 230 cm^{-1} at pH 2 and 260 cm^{-1} at pH 12.

A reasonable (albeit qualitative) measure of the splitting is also the total half-width of the band. It amounts to 670 cm^{-1} in $Al(OH)PcS_1$, 640 cm^{-1} in $Al(OH)PcS_2$, 680 cm^{-1} in $Al(OH)PcS_3$, and only to 500 cm^{-1} in $Al(OH)PcS_4$.

Besides the principal features mentioned above, a few less prominent ones can be distinguished in the spectra including a long-wavelength satellite of the Soret band around 380–400 nm, a wing at ca. 540–590 nm, and a feature appearing in some spectra beyond 700 nm.

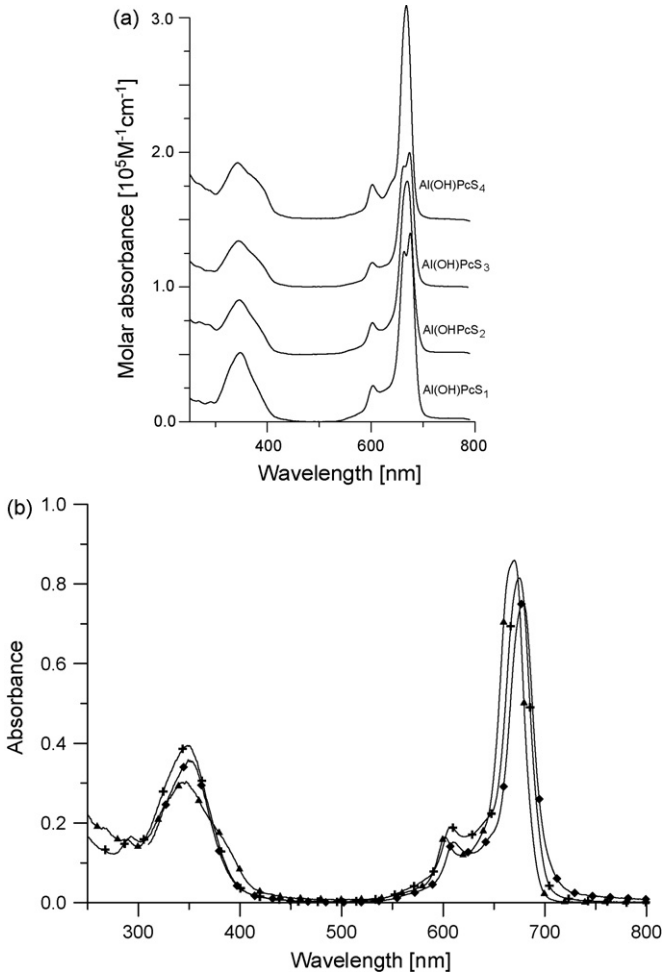

Fig. 2. (a) Absorption spectra of aqueous solutions of the sulfonated hydroxyaluminum phthalocyanines, measured at pH 12. The spectra of $Al(OH)PcS_2$, $Al(OH)PcS_3$ and $Al(OH)PcS_4$ have been vertically displaced. (b) pH dependence of absorption spectra of $Al(OH)PcS_2$ solutions (phosphate buffer). The concentration was equal to 8×10^{-6} M. Diamonds: pH 2; crosses: pH 7; triangles: pH 12.

3.2. Emission spectra and lifetimes of excited states

The emission and excitation spectra of $Al(OH)PcS_2$ and $Al(OH)PcS_3$ dissolved in a 1:1 mixture of methanol and 0.1 M NaOH (pH 12) are shown in Fig. 3.

The spectra of the remaining two phthalocyanines have also been measured but are not reproduced here as they contain no features other than those shown in the figure. The fluorescence spectra were found independent of the wavelength of the exciting light within the range employed in our experiments and are very similar for all $Al(OH)PcS_i$. At room temperature and in a 1:1 mixture of methanol and 0.1 M NaOH (pH 12), the peaks appeared at 678.0 nm for $Al(OH)PcS_1$; 673.6 nm for $Al(OH)PcS_2$; 676.6 nm for $Al(OH)PcS_3$ and 676.6 nm for $Al(OH)PcS_4$. It should be noted that the positions of the peaks depended on pH of the solvent: in pure water the respective wavelengths amounted to 684.4 nm for $Al(OH)PcS_1$ and $Al(OH)PcS_2$, 685.8 nm for $Al(OH)PcS_3$, and 682.2 nm for $Al(OH)PcS_4$. The peak positions were found slightly temper-

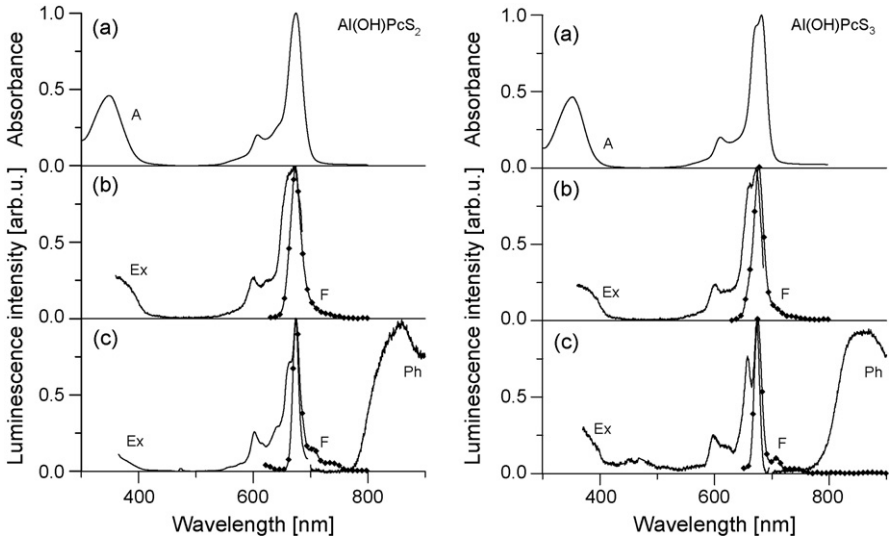

Fig. 3. Absorption and emission spectra in solutions of $Al(OH)PcS_2$ (left) and $Al(OH)PcS_3$ (right) in 1:1 mixture of methanol and 0.1 M NaOH (pH 12). (a) Absorption spectra at room temperature; (b) emission and excitation spectra at room temperature: F—fluorescence (excitation at 610 nm), Ex—fluorescence excitation spectrum (emission at 710 nm); (c) emission and excitation spectra at 77 K: F—fluorescence (excitation at 610 nm), Ph—phosphorescence (excitation at 315 nm), Ex—fluorescence excitation spectrum (emission at 710 nm). The spectra have been normalized to their peak values.

ature dependent: at 77 K and in the 1:1 mixture of methanol and 0.1 M NaOH (pH 12), the peak maxima are located at 679.8; 674.6; 675.4 and 675.8 nm, respectively. In all phthalocyanines and all solvents, only single bands were observed, due to purely electronic transitions. Additionally, well-resolved vibrational satellites were detected in 77 K spectra. The half-width of the fluorescence bands in $Al(OH)PcS_i$ were almost twice lower than the respective values in the absorption and excitation spectra, ranging between 420 and 475 cm^{-1} at room temperature, and between 320 and 365 cm^{-1} at 77 K.

The fluorescence excitation spectrum reproduces the absorption spectrum to within ca. 30 cm^{-1}. It is important to note that only bands due to monomers appear in the excitation spectra as the dimers are non-emissive. The half-widths of the bands in the excitation spectra roughly corresponded to those in the absorption spectra, ranging between 555 and 790 cm^{-1} at room temperature, and between 540 and 660 cm^{-1} at 77 K. At 77 K, where the spectra are better resolved, one may clearly notice a splitting of the Q band, even in $Al(OH)PcS_4$, where one would expect D_{4h} symmetry. In reality, presence of the OH group, inclined with respect to the molecular plane lowers the symmetry. The splitting amounts to ca. 250 cm^{-1} in even phthalocyanines and ca. 350 cm^{-1} in the odd ones.

The Stokes shift in all investigated compounds was found remarkably small, amounting to (95 ± 5) cm^{-1} at room temperature and no more than a few cm^{-1} at 77 K, at the concentrations used in this work (10^{-6} to 10^{-5} M). Such a small value of the Stokes shift affects the concentration dependence of the peak positions: between 10^{-6} and 10^{-4} M, the maxima move by ca. 400 cm^{-1} (cf. Fig. 4).

The phosphorescence in all phthalocyanines under investigation is much weaker than fluorescence; the low temperature phosphorescence intensity appeared 3–4 orders of magnitude below the fluorescence level. The phosphorescence spectra consist of broad bands, starting at ca. 780 nm and peaking at ca. 850 nm, apparently hiding some structure (cf. Fig. 3c). The singlet–triplet splitting may be estimated to amount to ca. 3000 cm^{-1}.

At the concentrations employed in our experiments (of the order of 10^{-7} to 10^{-6} M), the fluorescence quantum yields of all

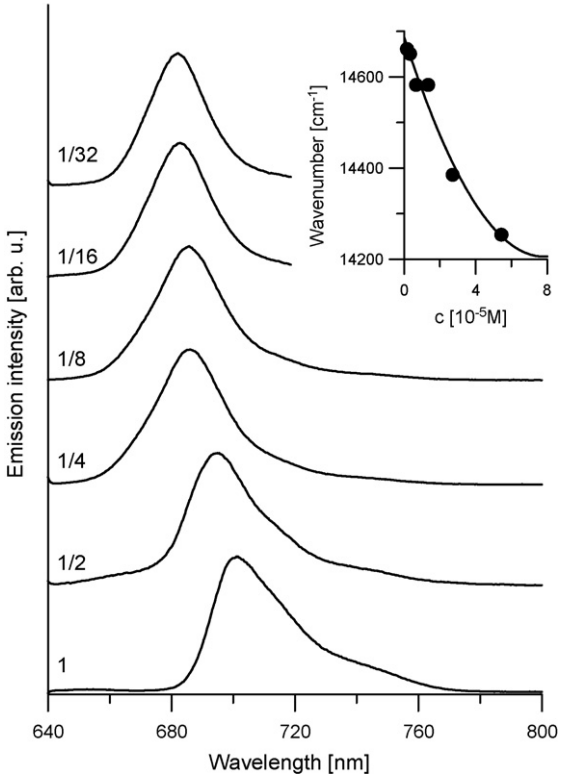

Fig. 4. Concentration dependence of the room-temperature fluorescence spectra of aqueous solutions of $Al(OH)PcS_2$ (pH 5.6). The numbers on the left side of the spectra denote fractions of the initial concentration equal to 5.46×10^{-5} M. Insert: concentration dependence of the peak maxima.

Table 2
Fluorescence quantum yields (Φ_F) and fluorescence lifetimes (τ_F) in aluminum phthalocyanines

Sample	Φ_F	τ_F (ns)
Al(OH)PcS$_1$[a]	0.45	5.35
Al(OH)PcS$_2$	0.67	4.96
Al(OH)PcS$_3$	0.52	5.01
Al(OH)PcS$_4$	0.74	5.25

The measurements were carried out in aqueous solutions of Al(OH)PcS$_2$, Al(OH)PcS$_3$ and Al(OH)PcS$_4$, and in a solution of Al(OH)PcS$_1$ in (1:1) mixture of methanol and 0.1 M NaOH (pH 12). The quantum yields are average values (error margin of ca. 10%), the lifetimes have been extrapolated to the infinite dilution.

[a] The value calculated for the lowest concentrations ($c < 7 \times 10^{-7}$ M).

Al(OH)PcS$_i$, except for Al(OH)PcS$_1$, were found concentration-independent. Due to insufficient solubility of Al(OH)PcS$_1$ in water, measurements in this case were carried out in alkaline solutions. In this system, the quantum yield was found to depend on concentration, decreasing with increasing concentration at concentrations exceeding ca. 5×10^{-7} M. Table 2 lists the quantum yields obtained from our experiments.

The fluorescence decays in all phthalocyanines under study proved nicely monoexponential up to the highest concentrations investigated (ca. 10^{-4} M); exemplary decays are shown in Fig. 5a and b. The fluorescence lifetimes depend on the dye concentration as is shown in Fig. 5c. The lifetimes, extrapolated to infinite dilutions, are given in Table 2.

The temporal evolution of the emission of singlet oxygen was measured for aqueous solutions of Al(OH)PcS$_3$ only (cf. Fig. 6). The measured curve is similar in shape to those reported in [16,22,23].

3.3. Dimer formation—reaction rates and equilibria

The absorption spectra shown in Section 3.1 are those of freshly prepared solutions. We found many spectra exhibit temporal changes, one of the reasons being the dimerization of the compounds under study. As the formation of aggregates strongly influences the photoactivity of phthalocyanines, the dimerization was studied in more detail. The process manifests itself as a decrease of the intensities of both the Soret band, the Q band and its vibrational satellite at 610 nm. The resulting increase of the dimer concentration gives rise to the buildup of the band at 640 nm and, possibly, of the weak wings below 590 nm and above 720 nm. In some cases a broad shoulder on the red edge of the Q band was seen, probably due to dimers and/or higher aggregates [24]. An exemplary set of spectra illustrating their evolution is shown in Fig. 7.

The changes of the spectra were found to crucially depend on pH of the solutions: no evolution could be observed in alkaline solutions, i.e., no aggregates were formed at high pH. It should be noted, however, that also in these solutions a band could be observed at ca. 630–640 nm. Thus we conclude that in the samples in which the dimerization does take place, the band is a superposition of a vibrational satellite of the monomer Q band (i.e., the band due to the ($S_0^{\upsilon=0} \rightarrow S_1^{\upsilon=1}$) transition), and a band due to a purely electronic transition in the dimer (when present). This conclusion is additionally supported by the analysis of the fluorescence excitation spectra (cf. Fig. 3), where the presence of the satellite is clearly visible.

More detailed studies of the dimerization could be carried out only for Al(OH)PcS$_2$ and Al(OH)PcS$_3$; among the two remaining phthalocyanines, Al(OH)PcS$_1$ exhibits a sufficient solubility only in alkaline solutions, and no measurable changes of the spectra were observed in Al(OH)PcS$_4$ at any pH. In the solutions in which the changes could be attributed to the dimerization (i.e., in which we observed a simultaneous decrease of the Q band and an increase of the 640 nm band), the temporal evolution of the intensities of the Q bands at their maxima could be reasonably well fitted with a second order kinetic equation. Moreover, analysis of the spectra allowed us to estimate the equilibrium constants of dimerization; the details will be presented in Section 4.

It should be noted, however, that in many samples the changes attributed to the dimer formation were apparently superimposed on another kinetic process: at low pH, absorbances were found slowly decreasing over the entire spectral range investigated. In these samples, visual inspection revealed formation of a sol, slowly precipitating from the solutions. On the other hand, in neutral and weakly alkaline solutions we sometimes observed a superposition of two processes, one associated with the dimer formation and another one manifesting itself in a slow buildup of the entire spectrum.

3.4. Quantum-chemical calculations

Structures of all sodium salts of Al(OH)PcS$_i$ were calculated. To mimic the situation of molecules in real solutions, the systems used in the calculations consisted of Al(OH)PcS$_i^{i-}$ anions and i hydrated Na^+ ions placed at the distance of 0.45 nm from the sulfonate groups. The distance chosen was estimated from the size of the hydrated sodium cation. The structure of Al(OH)PcS$_1$ monomer is shown in Fig. 8a. The organic part of the molecule is nearly planar, with the central metal atom located ca. 0.57 Å out of the plane formed by the organic rings.

The calculations of the structure of dimers were limited to Al(OH)PcS$_1$, and to Al(OH)Pc without sulfonate groups, used as a reference. There are two possibilities of the dimer formation as is shown in Fig. 8: the constituent molecules may be linked by either a hydrogen bond (HB) [25] or by an Al–O–Al bridge [26]. Structures of both these forms were investigated. The molecular planes of constituent molecules are parallel, with the interplanar distances amounting to 7.06 Å in the HB dimer, and to 4.52 Å in the Al–O–Al bridge dimer. Note that in both cases the interplanar distances are significantly longer than a typical π–π distance (3.35 Å). We therefore conclude that the π–π interaction does not play a significant role in the formation of dimers of Al(OH)PcS$_i$.

The calculations performed for isolated (non-solvated) molecules showed that the both forms should be stable: the total energy of the HB dimer is lower than the energy of the pair of monomers by ca. 23 kJ mol^{-1}, whereas the respective energy difference for the direct-bonding dimer amounts to ca. −2.2 kJ mol^{-1}. These energies can be additionally modified by

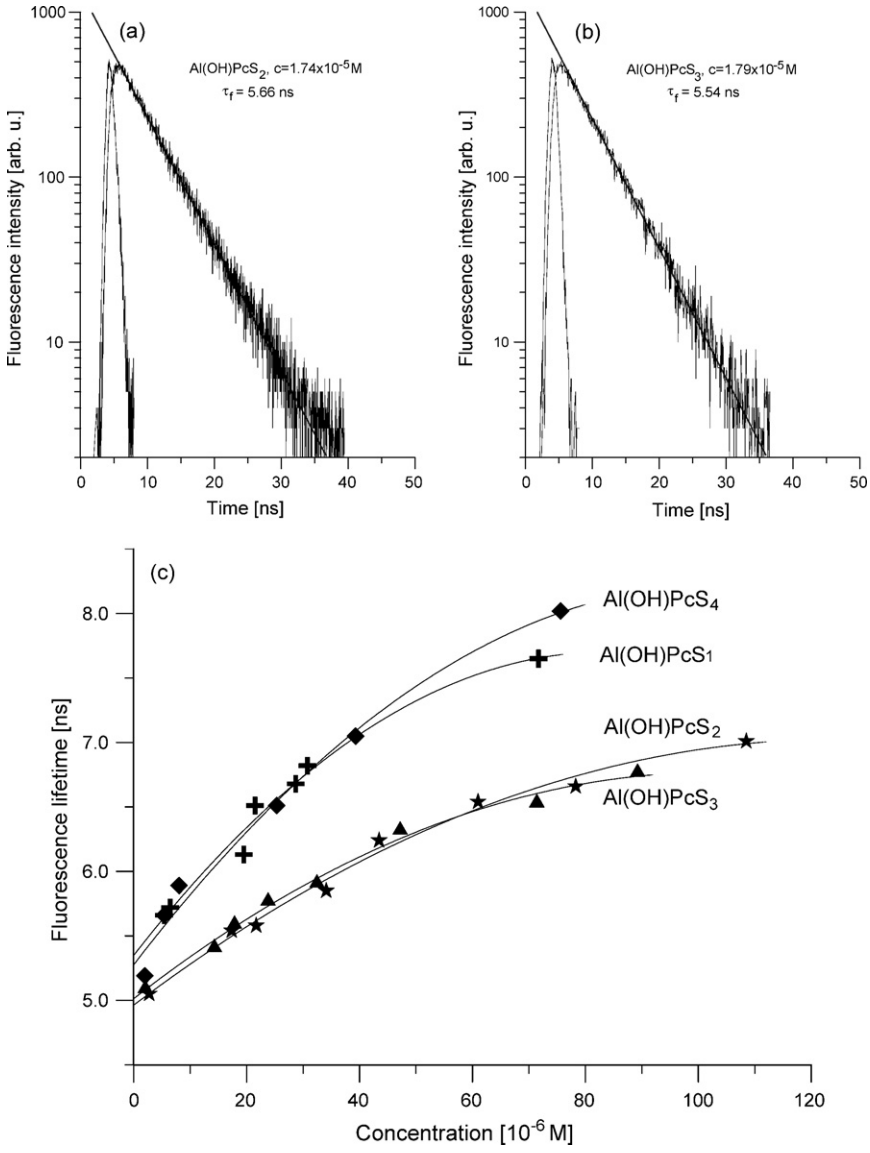

Fig. 5. Fluorescence decays in Al(OH)PcS_2 (a) and Al(OH)PcS_3 (b). The curves shown in the figure were measured in water solutions (pH 5.6). The concentrations are marked on the graphs. (c) Concentration dependences of the singlet lifetimes in solutions of sulfonated hydroxyaluminum phthalocyanines. Crosses: Al(OH)PcS_1; asterisks: Al(OH)PcS_2; triangles: Al(OH)PcS_3; diamonds: Al(OH)PcS_4. The solvents were 1:1 mixture of aqueous solution of NaOH and CH_3OH (pH 12) for Al(OH)PcS_1, and water (pH 5.6) for the remaining phthalocyanines.

the solvation. One can thus suppose that both forms can co-exist in solutions in various proportions depending on the nature of solvent and experimental conditions.

The HB dimer maintains nearly all features of the monomer molecule; in particular, the out of plane shift of the Al atom and Al–O bond length remain unchanged. The respective values in the other dimer also do not differ too much, amounting to 0.54 and 1.71 Å, respectively.

As was mentioned in Section 2.2, energies of electronic transitions were calculated using both, *ab initio* (TDDFT) and semi-empirical (GRINDOL) methods. In some cases, however, when the *ab initio* method could not be employed, we had to rely on the semi-empirical method only. It should be stressed, however, that whenever both methods could be used, the results obtained were reasonably similar. In the following, we shall present mainly results obtained from the semi-empirical method.

The results of calculations of the transition energies and oscillator strengths of all phthalocyanines are given in Table 3. As was already mentioned in this paper, two isomers can exist in Al(OH)PcS_2 differing in the positions of the sulfonate groups (in the opposite rings, hereafter referred to as *trans*-Al(OH)PcS_2, and in the adjacent rings, referred to as *cis*-Al(OH)PcS_2); the calculations were performed for both forms.

Energies of electronic transitions in the dimers of Al(OH)PcS_i have also been calculated. Table 4 presents selected results. For comparison, calculations have also been carried out for non-sulfonated Al(OH)Pc and its two dimers.

4. Discussion

Our results reported in the preceding section demonstrate a good agreement of the absorption spectra with those reported

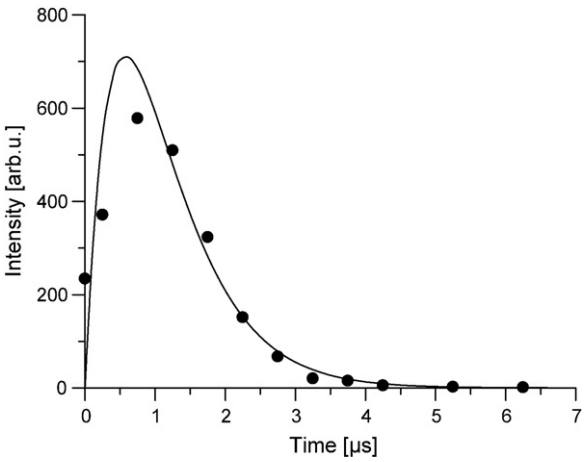

Fig. 6. Temporal evolution of the emission of singlet oxygen created in aqueous solutions of Al(OH)PcS_3. The emission intensity was measured at 1280 nm, at room temperature. The asterisks denote experimental points, the continuous line was calculated from Eq. (4), assuming the triplet lifetime of Al(OH)PcS_3 equal to 0.6 μs and the singlet lifetime of O_2 amounting to 0.6 μs.

earlier in the literature (e.g. [24]). It should be noted, however, that so far the spectra were reported for Al(OH)PcS_2 and Al(OH)PcS_4 where, for reasons of symmetry, no splitting of the Q band was observed in the room temperature spectra ([12,24,27–31], see also Fig. 2a). We report on results obtained on the entire series of sulfonated aluminum phthalocyanines.

The absorption spectra undergo temporal changes due mainly to the dimerization of the molecules in solutions. A quantitative

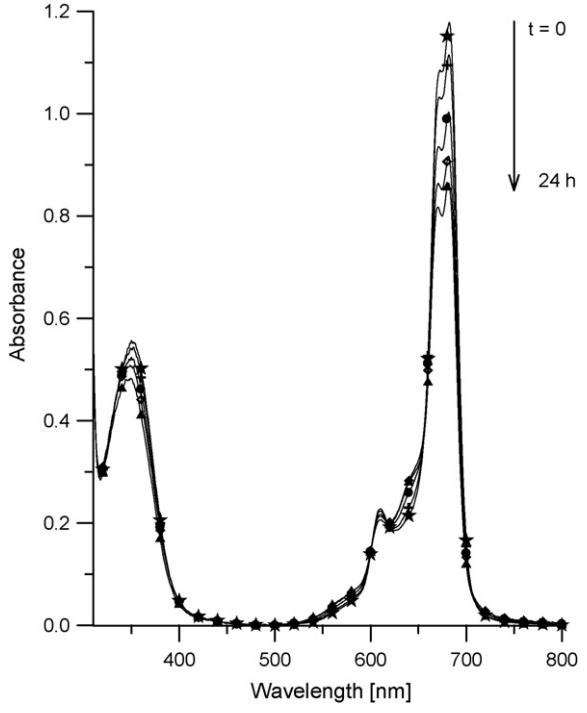

Fig. 7. Temporal changes of the absorption spectrum of Al(OH)PcS_3 in a pH 4 buffer. Asterisks: $t = 0$; crosses: $t = 15$ min; circles: $t = 60$ min; diamonds: $t = 150$ min; triangles: $t = 24$ h.

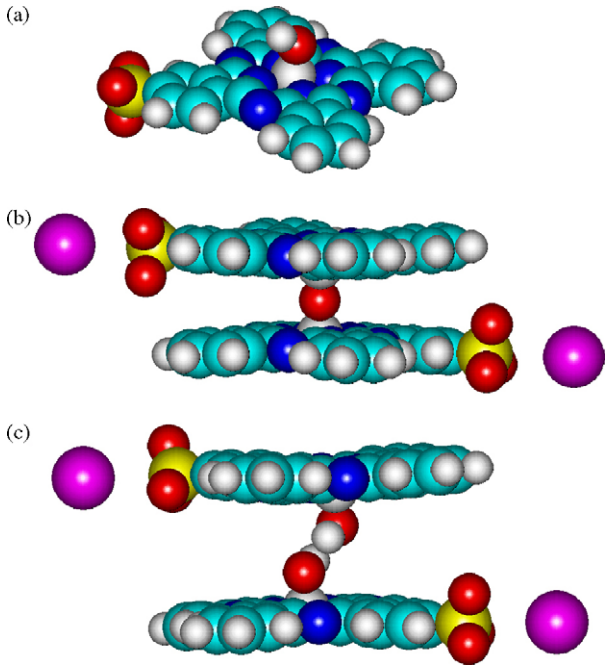

Fig. 8. Structures of the monomer anion (a), and of two possible dimers (b), (c) of Al(OH)PcS_1 (with cations indicated).

analysis of this process will be presented in the subsequent part of this section; here, we only state that the process occurs only in acidic and neutral solutions. A qualitative explanation seems obvious: the molecules are fully dissociated in alkaline solutions, and a strong electrostatic repulsion prevents aggregation of the molecules. Moreover, it should also be noted that our results seem to indicate that Al(OH)PcS_4 does not dimerize or dimerizes to a degree below our detectability level.

The dimer bands overlap with the vibrational satellites of the monomer (cf. Fig. 7) thus making a precise analysis rather complex. The presence of the satellites is, however, confirmed by the low temperature excitation spectra (Fig. 3) where no spectral features of the dimer should appear.

The low temperature excitation spectra clearly show a splitting of the Q band in all phthalocyanines under study, irrespective of their nominal symmetry. The splitting can be attributed to a loss of symmetry of the molecules caused by the sulfonation on their periphery and/or by the ligation with solvent molecules. At room temperature, the splitting is observed only in the lower-symmetry molecules, both in the absorption and excitation spectra. A similar Q-band splitting into Q_x and Q_y components (ca. 200 cm^{-1}) was observed in fluorescence excitation spectra Al(Cl)PcS_4 in various hyperquenched glassy solvents at 4.6 K [32].

Our experiments indicated that fluorescence is quite an efficient channel of deactivation of excited states. The fluorescence lifetimes determined for all materials under study are typically of the order of a few nanoseconds (ca. 5 ns when extrapolated to infinite dilution), increasing with concentration. The concentration changes of the fluorescence lifetimes observed in our experiments (cf. Fig. 5c) can be explained taking into account reabsorption and subsequent reemission of the emitted radiation as was discussed in [24].

Table 3
Electronic transition energies (ΔE, cm^{-1}), band splittings and oscillator strengths (f) in Al(OH)PcS$_i$

	ΔE_{calc} (Q band)	Splitting	f	ΔE_{calc} (Soret band)	Splitting	f	ΔE_{exp} (Q band)	Splitting (Q band)
Al(OH)PcS$_1^-$ + Na$^+$	14111	241	0.493	29878	86	1.130	14805	255
	14352		0.520	29964		1.052	15060	
trans-Al(OH)PcS$_2^{2-}$ + 2Na$^+$	14253	272	0.539	30317	350	0.917	14925	
	14525		0.544	30667		1.049		
cis-Al(OH)PcS$_2^{2-}$ + 2Na$^+$	14466	456	0.537	30107	247	0.773		
	14922		0.550	30354		0.977		
Al(OH)PcS$_3^{3-}$ + 3Na$^+$	15057	152	0.606	30637	482	1.132	14837	280
	15209		0.640	31119		0.714	15117	
Al(OH)PcS$_4^{4-}$ + 4Na$^+$	15326	49	0.625	31695	345	1.118	14981	
	15375		0.625	32040		0.784		

The experimental values of ΔE and splitting are given for comparison.

The fluorescence quantum yields are quite high, ranging between ca. 0.4 and 0.7 in diluted aqueous solutions of Al(OH)PcS$_2$, Al(OH)PcS$_3$ and Al(OH)PcS$_4$, and in alkaline solutions of Al(OH)PcS$_1$, in agreement with literature data [30,33,34] (cf. Table 2).

It is instructive to compare the natural lifetimes of the singlet states (τ_0) in the phthalocyanines under study, determined from the experimental results with those obtained from the quantum chemical calculations. The latter parameter can be calculated from the equation [35]

$$\tau_0 = \frac{m_e \varepsilon_0 c_0}{2\pi e^2 \tilde{\nu}_{max}^2 n f} \quad (2)$$

where m_e and e are electron mass and charge, ε_0 is the permittivity of free space, c_0 is the speed of light *in vacuo*, n is the refractive index of the medium, $\tilde{\nu}_{max}$ is the wavenumber corresponding to the absorption maximum, and f is the oscillator strength (all expressed in SI units). Expressing the wavenumber to practical units (cm^{-1}) and remembering that the calculations were carried out for isolated molecules, one arrives at the equation often cited in the literature (e.g. [36])

$$\tau_0 = \frac{1.5}{\tilde{\nu}_{max}^2 f} \quad (2a)$$

The natural lifetime can also be determined from the experimental data using the equation

$$\tau_0 = \frac{\tau_f}{\varphi_f} \quad (3)$$

where τ_f is the singlet lifetime determined from the experiment and φ_f is the experimental fluorescence quantum yield (cf. Table 2). A comparison of the natural lifetimes is shown in Table 5.

The agreement between the calculated and experimental data (which may be taken as an additional consistency test of our calculations) is satisfactory in the case of Al(OH)PcS$_2$ and quite good for Al(OH)PcS$_1$, Al(OH)PcS$_3$ and Al(OH)PcS$_4$.

Our results indicate that the triplet state in Al(OH)PcS$_2$ and Al(OH)PcS$_3$ is located close to 780 nm (i.e., at ca. 1.6 eV; cf. Fig. 3). As the location of the S_1 state does not practically depend on the number of sulfonate groups, one may presume that the triplet state energy in other phthalocyanines under study is the same. Due to a very weak signal, the triplet state lifetimes could not be determined reliably, and could be estimated only indirectly (cf. Fig. 6), from a fit to the temporal evolution of the singlet oxygen emission.

Assuming that singlet oxygen is produced in a Type II reaction (cf. Fig. 1a), the scheme depicting the production and decay

Table 4
Calculated values of electronic transition energies (ΔE, cm^{-1}), oscillator strengths (f) and the splittings of the Q bands in Al(OH)PcS$_i$

	ΔE_{calc}	f	Splitting
Monomer Al(OH)Pc	14200	0.506	46
	14246	0.503	
Dimer (AlPc)$_2$=O	13100	0.000	1840
	13100	0.000	
	14940	0.766	
	14940	0.766	
Dimer (Al(OH)Pc)$_2$	13685	0.000	910
	13751	0.000	
	14603	0.884	
	14648	0.877	
Dimer ((Al(OH)PcS$_1$)$_2$=O)$^{2-}$ + 2Na$^+$	13170	0.000	2020
	13388	0.000	
	15207	0.861	
	15396	0.816	
Dimer (Al(OH)PcS$_1$)$_2^{2-}$ + 2Na$^+$	14002	0.000	970
	14385	0.000	
	15025	1.015	
	15300	0.996	

Table 5
A comparison of the singlet natural lifetimes in phthalocyanines under study

Molecule	$\tau_{0,calc}$ (ns)	$\tau_{0,exp}$ (ns)	k_f ($\times 10^8$ s^{-1})
Al(OH)PcS$_1$	15	13	0.8
trans-Al(OH)PcS$_2$	14	7	1.4
cis-Al(OH)PcS$_2$	13		
Al(OH)PcS$_3$	11	10	1.0
Al(OH)PcS$_4$	10	7	1.4

The input data for $\tau_{0,calc}$ are given in Table 3, the experimental data used in calculations of $\tau_{0,exp}$ are given in Table 2. The fluorescence rate constants (k_f) were calculated from the experimental data.

of $^1O_2$ can be written schematically as

$$^3Pc^* + {}^3O_2 \xrightarrow{k_a} {}^1Pc^0 + {}^1O_2^* \xrightarrow{k_b} {}^1Pc^0 + {}^3O_2$$

The process, under an excess of ground state reactants, should follow first order kinetics, the solution for the temporal evolution the concentration of $^1O_2$ being [35]

$$c(^1O_2^*) = c(^3Pc^*)\frac{k_a}{k_b - k_a}[\exp(-k_a t) - \exp(-k_b t)] \quad (4)$$

where k_a and k_b are rate constants of the elementary processes. The fit to the experimental points, shown in Fig. 6, yields $k_a = 1.73 \times 10^6\ s^{-1}$, $k_b = 1.74 \times 10^6\ s^{-1}$. One may thus conclude that, to within experimental uncertainty, both time constants are equal and close to ca. 0.6 μs, substantially shorter than the values reported in [7,33] but similar to those determined in similar systems (porphines) [16,22,23]. The reason for the discrepancy may be sought in presence of oxygen in our samples: it is known [37] that oxygen substantially shortens the triplet lifetimes. This factor, however, is to be investigated in detail.

Due to a very weak signal, our results reporting on the singlet oxygen emission should be treated with some caution but we can state that the singlet oxygen lifetime is below 1 μs in aqueous solutions of Al(OH)PcS_3. This value is a few times shorter than the values reported for porphines [16,22,23,38], and nearly 3 orders of magnitude below the values reported in for tetra-*tert*-butyl metal-free Pc [39] in C_6D_6. It is known, however, that the singlet oxygen lifetime depends strongly on the solvent (cf., e.g. [38]) and the presence of photoactive molecules dissolved in them [37].

An important question that should be answered is the nature of aggregates formed by the phthalocyanines under study. One can envisage formation of two types of dimers: a pair of hydrogen-bonded molecules [25] and a dimer connected via an Al–O–Al bond [26]. The former species seems to be spectrally indistinguishable from the monomer [25,40], differing, however, in molar absorbances of solutions. Thus the formation or annihilation of such aggregates, possibly also associated with other equilibria involving sulfonate groups [31], may account for the changes the absorbances of entire spectra mentioned in Section 3.3, as well as for a slight shift of the peaks in function of pH (cf. Fig. 2b). It is important to note, however, that – irrespective of the nature of the dominating dimers – the arrangement of the constituent molecules is that as in H aggregates. Thus one should expect spectral behaviour of the dimers characteristic of H aggregates.

As was mentioned above, the quantum chemical calculations were performed for non-sulfonated dimer and for Al(OH)PcS_1 only. Thus the discussion will be related to these two species only. Our calculations (cf. Table 4) locate the band due to the hydrogen-bonded dimer at 660 nm, whereas the band of the Al–O–Al bridged dimer should appear at ca. 653 nm. The corresponding values for the non-sulfonated dimer amount to 684 and 661 nm, respectively. Taking into account an unavoidable uncertainty of the calculations, these results, compared with experimental data (cf. Fig. 2a and Table 4), do not allow us to decide which type of dimer prevails in the systems under

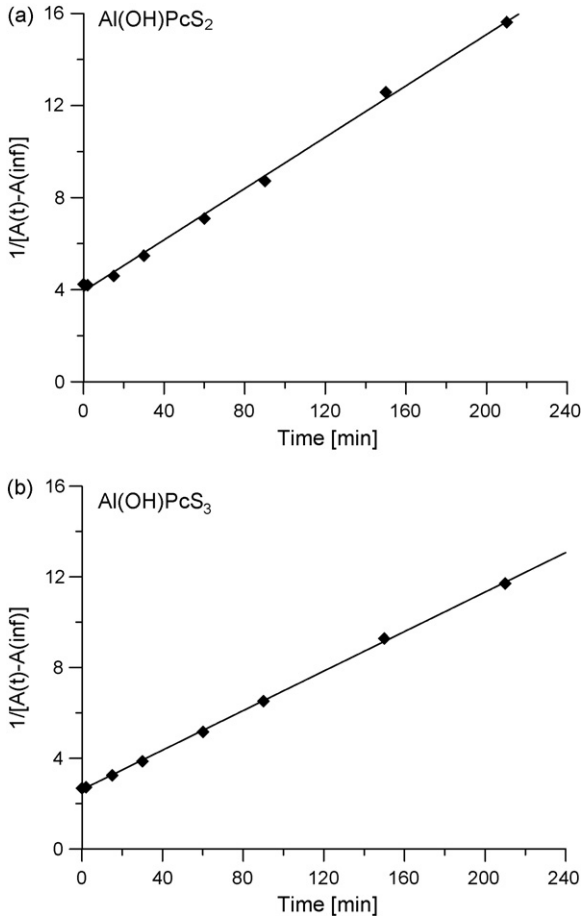

Fig. 9. Intensities of the Q band in Al(OH)PcS_2 and Al(OH)PcS_3 dissolved in a buffer (pH 4), plotted in the co-ordinates resulting from Eq. (12).

study. In the subsequent discussion, we shall presume that the direct-bonded dimer is formed but it should be stressed that all equations derived in the subsequent part of this section (and hence all results) are independent of the dimerization reaction assumed.

The reaction can be written as

$$2M \underset{k_2}{\overset{k_1}{\rightleftharpoons}} D + H_2O$$

Let a and b stand for the initial concentrations of the monomer (M) and dimer (D), respectively, x for the concentration of the dimer produced since the beginning of the reaction, and k_1 and k_2 for rate constants of the elementary reactions. Then the kinetic equation can be written as

$$\frac{dx}{dt} = k_1(a - 2x)^2 - k_2(b + x) \quad (5)$$

The (dimensionless) equilibrium constant of the dimerization, K_d, defined as

$$K_d = \frac{(b + x_{eq})c^0}{(a - 2x_{eq})^2} \quad (6)$$

Table 6
Second order rate constants and equilibrium constants of dimerization of sulfonated hydroxyaluminum phthalocyanines

pH	$Al(OH)PcS_2$			$Al(OH)PcS_3$		
	c ($\times 10^{-6}$ M)	k_1 ($M^{-1}\,s^{-1}$)	K_d	c ($\times 10^{-6}$ M)	k_1 ($M^{-1}\,s^{-1}$)	K_d
4	7.6	14	3.2×10^4	11.8	12	5.8×10^4
	8.3	13	4.8×10^4	11.2	6	2.6×10^4
	10.2	11	2.6×10^4	6.0	18	3.6×10^4
5	7.1	28	4.0×10^4	9.6	8	2.8×10^4
5.6	7.5	11	0.3×10^4			
6	6.4	16	0.6×10^4			

is related to the rate constants by a simple relation

$$K_d = \frac{k_1 c^0}{k_2} \tag{7}$$

In the above equations, the concentrations are expressed in M, $c^0 = 1$ M, and the subscript eq denotes equilibrium conditions. Since only diluted solutions are considered, the concentration of water was assumed constant and included in k_2.

A general solution of Eq. (5) reads

$$\ln\frac{x_1(x_2 - x)}{x_2(x_1 - x)} = k_{eff}t \tag{8}$$

where

$$x_{1,2} = \frac{1}{2}\left[a + \frac{c^0}{4K_d}\left(1 \pm \sqrt{1 + 8K_d\frac{c}{c^0}}\right)\right] \tag{9}$$

$$k_{eff} = k_2\sqrt{1 + 8K_d\frac{c}{c^0}} \tag{10}$$

and c is the total concentration of phthalocyanine. If, however, $K_d \gg 1$ (i.e., if $x_1 \approx x_2 \approx a/2$) and $b \ll a$, the solution is typical of a second order reaction

$$\frac{1}{a - 2x} - \frac{1}{a} = 2k_1 t \tag{11}$$

Making use of the Lambert–Beer law, one arrives at the final equation

$$\frac{1}{A_t - A_\infty} = \frac{1 + 2ak_1 t}{A_0 - A_\infty} \tag{12}$$

Eq. (12) was used to fit experimental data obtained for those solutions in which a simultaneous decrease of the intensity of the Q band and an increase of the intensity at 640 nm was observed. Exemplary results are shown in Fig. 9, and the results obtained are listed in Table 6.

Simultaneously, the values of A_0 and A_∞ were used to calculate the equilibrium constant. After suitable transformation, Eq. (6) becomes

$$K_d = \frac{A_0 - A_\infty}{A_\infty^2}\varepsilon c^0 L \tag{13}$$

where ε is the molar absorbance and L stands for the cuvette thickness. The results obtained for $Al(OH)PcS_2$ and $Al(OH)PcS_3$ are given in Table 6.

Despite a significant spread, the results obtained seem to indicate that K_d decreases with increasing pH of the solutions whereas, within the experimental accuracy, the rate constant of dimerization remains constant. Our values of the dimerization constant are approximately two orders of magnitude lower than those reported in [27,31] for $Al(OH)PcS_2$ in aqueous solutions (phosphate buffers). We cannot offer a convincing explanation of these discrepancies but it seems that the answer should be sought in different methods of treating the experimental data: our results have been calculated from the analysis of temporal evolution of the spectra, whereas the results reported in [27,31] were obtained from steady state experiments performed on solutions of different concentrations. Moreover, our observations indicate (cf. Section 3.3) that it is conceivable to suppose that the results reported in [27,31] were obscured by the formation of sols at low pH and higher concentrations.

It is interesting to note that the ratio of intensities of the Q and Soret bands seems to be a good (albeit qualitative) indicator of the state of aggregation. In freshly prepared alkaline solutions of $Al(OH)PcS_4$ (pH 12), where the dimerization can be practically ruled out, the ratio amounts to 3.6 ± 0.1; in the same conditions, the ratio amounts to 3.0 ± 0.1 for $Al(OH)PcS_3$ and $Al(OH)PcS_2$, and to 2.7 ± 0.1 for $Al(OH)PcS_1$. At pH 7, the respective ratios amount to 3.0; 2.2; 2.1 and 2.7. The dimerization results in a further decrease of the ratios.

5. Conclusions

Photophysical properties of photodynamic sensitizers, sodium salts of hydroxyaluminum phthalocyanine sulfonates containing 1 to 4 sulfonate groups, were studied. Measurements of temporal evolution of UV–vis absorption spectra point to the dimerization of $Al(OH)PcS_2$ and $Al(OH)PcS_3$ in acidic solutions. The second order rate constants of the dimerization are of the order of $10\,M^{-1}\,s^{-1}$, the equilibrium constants of the order of 10^4 at pH 4 and probably decrease with increasing pH.

Major spectral features of the compounds under study seem to be only weakly affected by the number of sulfonate groups. The fluorescence quantum yields are high (up to 0.74), depending on the number of sulfonate groups. The singlet lifetimes are of the order of a few nanoseconds which may be considered typical values, the triplet lifetimes, however, appear quite short in comparison with the values reported in the literature.

The results reported in this paper do not provide a direct answer to the question concerning applicability of hydroxya-

luminum phthalocyanine sulfonates in photodynamic therapy. However, taking into account a total of properties of the compounds under examination (solubility in water and physiological solutions, quantum yield of fluorescence, dimer formation, etc.), only Al(OH)PcS_1 appears unsuitable. The efficiency of the remaining phthalocyanines in production of singlet oxygen and oxygen superradicals should, however, be examined.

Acknowledgements

The work was supported by the Wrocław University of Technology, and by the Grant No. KAN400720701 from the Academy of Sciences of the Czech Republic. The authors would like to thank Prof. J. Hála (Charles University Prague). and Dr. G. Wang (China National Institute of Standardization Beijing) for their help with the flash photolysis measurements, and Dr. S. Böhm (Prague Institute for Chemical Technology) for useful discussions concerning quantum chemical calculations.

References

[1] D.J. McGarvey, T.G. Truscott, in: D. Kessel (Ed.), Photodynamic Therapy of Neoplastic Diseases, vol. 1, CRC Press, Boca Raton, FL, 1990, pp. 179–189.
[2] S.G. Bown, J. Photochem. Photobiol. B: Biol. 6 (1990) 1–12.
[3] T. Hasan, B. Ortel, A.C.E. Moor, B.W. Pogue, Photodynamic therapy of cancer, in: Holland-Frei Cancer Medicine, 6th ed., B.C. Decker Inc., Hamilton, Ont., 2003, pp. 605–622 (Chapter 40).
[4] H. Barr, C.J. Tralau, P.B. Boulos, A.J. MacRobert, R. Tilley, S.G. Bown, Photochem. Photobiol. 46 (1987) 795–800.
[5] M. Ambroz, A.J. MacRobert, J. Morgan, G. Rumbles, M.S.C. Foley, D. Phillips, J. Photochem. Photobiol. B: Biol. 22 (1994) 105–117.
[6] M.C. DeRosa, R.J. Crutchley, Coord. Chem. Rev. 233/234 (2002) 351–371.
[7] D. Phillips, Pure Appl. Chem. 67 (1995) 117–126.
[8] V.S. Chan, J.F. Marshall, R. Svensen, D. Phillips, I.R. Hart, Photochem. Photobiol. 45 (1987) 757–761.
[9] J.R. Darwent, P. Douglas, A. Harriman, G. Porter, M.-C. Richoux, Coord. Chem. Rev. 44 (1982) 83–126.
[10] P.S. Vincett, E.M. Voigt, K.E. Rieckhoff, J. Chem. Phys. 55 (1971) 4131–4140.
[11] J.R. Wagner, H. Ali, R. Langlois, N. Brasseur, J.E. van Lier, Photochem. Photobiol. 45 (1987) 587–594.
[12] A. Ogunsipe, T. Nyokong, Photochem. Photobiol. Sci. 4 (2005) 510–516.
[13] J. Moan, Q. Peng, An outline of the history of PDT, in: T. Patrice (Ed.), Photodynamic Therapy. Comprehensive Series of Photochemical and Photobiological Sciences, RSC Publ., London, 2003, pp. 3–37.
[14] J.C. Scaiano (Ed.), Handbook of Organic Photochemistry, CRC Press, Boca Raton, FL, 1989.
[15] A Guide to Recording Fluorescence Quantum Yields, www.jobinyvon.com/read.asp?Docid=1546.
[16] R. Dědic, A. Svoboda, J. Pšenčík, J. Hála, J. Mol. Struct. 651–653 (2003) 301–304.
[17] J.A. Pople, D.L. Beveridge, P. Dobosh, J. Chem. Phys. 47 (1967) 2026.
[18] M.J. Frisch, G.W. Trucks, H.B. Schlegel, G.E. Scuseria, M.A. Robb, J.R. Cheeseman, J.A. Montgomery Jr., T. Vreven, K.N. Kudin, J.C. Burant, J.M. Millam, S.S. Iyengar, J. Tomasi, V. Barone, B. Mennucci, M. Cossi, G. Scalmani, N. Rega, G.A. Petersson, H. Nakatsuji, M. Hada, M. Ehara, K. Toyota, R. Fukuda, J. Hasegawa, M. Ishida, T. Nakajima, Y. Honda, O. Kitao, H. Nakai, M. Klene, X. Li, J.E. Knox, H.P. Hratchian, J.B. Cross, V. Bakken, C. Adamo, J. Jaramillo, R. Gomperts, R.E. Stratmann, O. Yazyev, A.J. Austin, R. Cammi, C. Pomelli, J.W. Ochterski, P.Y. Ayala, K. Morokuma, G.A. Voth, P. Salvador, J.J. Dannenberg, V.G. Zakrzewski, S. Dapprich, A.D. Daniels, M.C. Strain, O. Farkas, D.K. Malick, A.D. Rabuck, K. Raghavachari, J.B. Foresman, J.V. Ortiz, Q. Cui, A.G. Baboul, S. Clifford, J. Cioslowski, B.B. Stefanov, G. Liu, A. Liashenko, P. Piskorz, I. Komaromi, R.L. Martin, D.J. Fox, T. Keith, M.A. Al-Laham, C.Y. Peng, A. Nanayakkara, M. Challacombe, P.M.W. Gill, B. Johnson, W. Chen, M.W. Wong, C. Gonzalez, J.A. Pople, Gaussian 03, Revision D.01, Gaussian Inc., Wallingford, CT, 2004.
[19] J. Lipinski, Int. J. Quantum Chem. 34 (1988) 423–435.
[20] J. Sworakowski, J. Lipiński, L. Ziółek, K. Palewska, S. Nešpůrek, J. Phys. Chem. 100 (1996) 12288.
[21] J. Lipiński, W. Bartkowiak, J. Phys. Chem. A 101 (1997) 2159.
[22] R. Dědic, A. Molnár, M. Kořinek, A. Svoboda, J. Pšenčík, J. Hála, J. Lumin. 108 (2004) 117–119.
[23] M. Kořinek, R. Dědic, A. Molnár, J. Hála, J. Fluoresc. 16 (2006) 355–359.
[24] S. Dhami, A.J. de Mello, G. Rumbles, S. Bishop, D. Phillips, A. Beeby, Photochem. Photobiol. 61 (1995) 341–346.
[25] N.A. Kuznetsova, N.S. Gretsova, V.M. Derkacheva, S.A. Mikhalenko, L.I. Solov'eva, O.A. Yuzhakova, O.L. Kaliya, E.A. Luk'yanets, Russ. J. Gen. Chem. 72 (2002) 300–306.
[26] K.J. Wynne, Inorg. Chem. 24 (1985) 1339–1343.
[27] Z. Petrášek, D. Phillips, Photochem. Photobiol. Sci. 2 (2003) 236–244.
[28] T.I. Rokitskaya, M. Block, Y.N. Antonenko, E.A. Kotova, P. Pohl, Biophys. J. 78 (2000) 2572–2580.
[29] M.O. Liu, C.-H. Tai, M.-Z. Sain, A. Teh Hu, F.-I. Chou, J. Photochem. Photobiol. A: Chem. 165 (2004) 131–136.
[30] S. Dhami, G. Rumbles, A.J. MacRobert, D. Phillips, Photochem. Photobiol. 65 (1997) 85–90.
[31] R.B. Ostler, A.D. Scully, A.G. Taylor, I.R. Gould, T.A. Smith, A. Waite, D. Phillips, Photochem. Photobiol. 71 (2000) 397–404.
[32] T. Reinot, J.M. Hayes, G.J. Small, M.C. Zerner, Chem. Phys. Lett. 299 (1999) 410–416.
[33] M.S.C. Foley, A. Beeby, A.W. Parker, S.M. Bishop, D. Phillips, J. Photochem. Photobiol. B: Biol. 38 (1997) 10–17.
[34] A.M. Ambroz, A. Beeby, A.J. MacRobert, M.S.C. Simpson, R.K. Svensen, D. Phillips, J. Photochem. Photobiol. B: Biol. 9 (1991) 87–95.
[35] H. Kuhn, H.-D. Försterling, Principles of Physical Chemistry. Understanding Molecules, Molecular Assemblies, Supramolecular Machines, J. Wiley, Chichester, 2000.
[36] M. Klessinger, J. Michl (Eds.), Excited States and Photochemistry of Organic Molecules, VCH, New York, 1995 (Chapter 5.1.2).
[37] A. Segalla, C.D. Borsarelli, S.E. Braslavsky, J.D. Spikes, G. Roncucci, D. Dei, G. Chiti, G. Jori, E. Reddi, Photochem. Photobiol. Sci. 1 (2002) 641–648.
[38] J. Mosinger, Z. Mička, J. Photochem. Photobiol. A: Chem. 107 (1997) 77–82.
[39] Y. Fu, A.A. Krasnovsky Jr., C.S. Foote, J. Phys. Chem. A 101 (1997) 2552–2554.
[40] D.A. Fernández, J. Awruch, L.E. Dicello, Photochem. Photobiol. 63 (1996) 784–792.